COMMUNICATION

Technology

Non-thermal, pulsed electric field cell ablation: A novel tool for regenerative medicine and scarless skin regeneration

Alexander Golberg[1], G. Felix Broelsch[2], Stefan Bohr[1,5], Martin C. Mihm, Jr.[3], William G. Austen, Jr.[2], Hassan Albadawi[4], Michael T. Watkins[4] & Martin L. Yarmush[1,6]

High voltage, short pulsed electric fields (PEF) is a non-thermal ablation method, in which defined PEF irreversibly destabilize cell membranes, while preserving other tissue components such as the extracellular matrix (ECM). In the present report, we show that PEF ablated rat skin retains its microvascular blood supply and ECM structure. Complete regeneration of epidermis, hair follicles, sebaceous glands, and the panniculus carnosusis observed two months after the ablation. Our results clearly indicate that non-thermal PEF has the potential to be a powerful and novel tool for scarless tissue regeneration.

INNOVATION

To date, scarless regeneration has only been observed in fetal wounds and amphibian models. Fetal wounds regenerate rapidly, notably without the characteristics of secondary defects such as scar formation. Although amphibian models for limb regeneration are well established, differences for example related to inflammation and immunity considerably reduce their relevance to the human condition. Thus, methodology to induce scarless adult wound healing in mammals is needed to better understand tissue regeneration processes and to develop new therapies that lead to improved cosmetic and functional results. In this study, we report on a scarless adult skin regeneration model in rats developed using non-thermal, pulsed electric fields (PEF) controlled ablation of cells. We show that PEF ablated skin preserves the microvascular blood supply and extracellular matrix structure. A complete regeneration of epidermis, hair follicles, sebaceous glands and the dermal panniculus carnosus was observed two months after non-thermal PEF ablation. These results suggest that PEF may become a key tool for regenerative medicine allowing for scarless healing following efficient and controlled ablation of cellular tissue components.

NARRATIVE

Wound healing in mammals is often accompanied by the presence and activity of highly specialized cell types, most notably fibroblastic phenotypes, which are responsible for the replacement of original tissue components with scar tissue. Though effective in maintaining overall tissue integrity, variations of this process, such as seen with hypertrophic scarring (HTS), can dramatically affect a patient's quality of life, both physically and psychologically. Thus, considerable efforts have been undertaken to unravel the mechanisms behind HTS in the hope of developing novel treatment strategies[1]. Several aspects of wound healing, i.e. coagulation phenomena, inflammation, angiogenesis, fibroplasia, wound contraction, tissue remodeling and mechanical tension, have been shown to correlate with the formation of more extensive HTS[2–4]. In this context, the importance of tissue structure and extracellular matrix (ECM) components on inflammatory or proliferative processes during wound healing has been a focus of attention in recent years[2–4]. However, the process of scar formation is still poorly understoodwith a pressing need for a novel approach to effectively treat skin pathologies such as HTS.

To date, a lack of valid animal models which correspond to adult human wound healing has been a major obstacle. Although considerable work over the last three decades has revealed that fetal wounds typically heal rapidly without scar formation[5], fetal wounds are very different from their adult counterparts with regard to ECM content, the inflammatory response, and angiogenesis. Thus, the results from fetal studies are not translatable to adult wound healing. To date, animal models of tissue regeneration and repair have focused on amphibians[6], rabbits[7], pigs[7] and small rodents[7]. However, the lack of an adaptive immune system in amphibians as well as the phenomenon of defect healing in rodents via active wound contraction using a

[1]Center for Engineering in Medicine, Department of Surgery, Massachusetts General Hospital, Harvard Medical School, and the Shriners Burns Hospital, Boston, MA 02114, USA. [2]Division of Plastic and Reconstruction Surgery, Massachusetts General Hospital, Harvard Medical School, Boston, MA 02114, USA. [3]Department of Dermatology, Brigham and Women's Hospital, Harvard Medical School, Boston, MA 02115, USA. [4]Division of Vascular and Endovascular Surgery, Massachusetts General Hospital, Harvard Medical School, Boston, MA 02114, USA. [5]Plastic and Hand Surgery Division — Burn Center, University Clinics RWTH Aachen, 52074 Aachen, Germany. [6]Department of Biomedical Engineering, Rutgers University, Piscataway, NJ 08854, USA. Correspondence should be addressed to M.L.Y. (ireis@sbi.org).

Received 14 June 2013; accepted 13 August 2013; published online 24 September 2013; doi:10.1142/S233954781320001X

specialized intradermal muscle (panniculus carnosus) counteract the translational intent aimed at generating novel concepts of treatment.

Recently, studies using controlled tissue ablation with pulsed electric fields (PEF) have shown promising results related to the potential of effective tissue regeneration in different organs[8]. One possible mechanisms of cell and tissue death after the exposure to PEF is irreversible electroporation — an irreversible increase of cell membrane permeability that leads to cell death. For example, PEF-ablated human liver showed reduced fibrosis compared to radio-frequency ablation in clinical trials[9]. In addition, scarless regeneration of the vascular system and small intestine were reported in rats and pigs[10,11]. Other studies demonstrated reduced scar formation with preservation of blood vessels and bile duct structures after PEF of both liver and pancreas in pigs[12,13]. These studies, however, were focused exclusively on PEF application for tumor ablation, rather than the phenomenon of scarless tissue regeneration, and thus reduced fibrosis was reported only as a favorable side-effect of PEF in comparison to other tissue ablation methods. Recently, we have successfully developed an intermittently delivered pulsed electric fields protocol that controls human normal skin fibroblasts density in culture[14]. We showed that in culture, the fraction of fibroblasts that survive the PEF regenerates to the 100% confluency[14]. Based on these prior observations, we set out to evaluate PEF as a novel tool for use in regenerative medicine. As indicated below, we demonstrated that non-thermal PEF can be used to generate effective models for studying mechanisms of wound healing, and that PEF application may actually generate scarless wound healing in adult mammals.

To demonstrate the use of non-thermal PEF ablation in the context of regenerative medicine, we investigated the outcome of skin regeneration following PEF skin ablation in rats. Using contact electrodes, we ablated an area of 1 cm^2 on the dorsal skin of female Sprague Dawley rats with non-thermal PEF (**Fig. 1a,b**). The following PEF parameters were used to minimize the thermal effects of pulsed electric fields on tissue: field strength (E) 500 V, 2 mm gap between electrodes, pulse duration (t_p) 70 µs, delivery frequency (f) 2 Hz, total number of pulses (N) 180. The pulses were delivered in 4 series of 45 pulses each with a pause of 30 s in betweenthe series. To estimate the thermal effects of PEF, we measured the currents generated during each pulse (**Fig. 1c**) and modeled Joule heating of the treated skin (details of the electro-thermal model appear inthe **Supplementary Information 1**). Heat supplied to the skin by each electric pulse is calculated as in Equation (1):

$$Q_n = I_n V t_p \tag{1}$$

where Q_n (in Joules) is the heat supplied to the skin by a single pulse (n); I_n (in Amps) is the current during the pulse number (n), V (in Volts) is the applied voltage. The temperature increase of a treated skin section, immediately after the application of E is calculated using Equation (2):

$$T_{pn} = \frac{Q}{mc_p} + T_{in} \tag{2}$$

where m (in kg) is the mass of a skin section on which electric fields are applied; c_p (J kg^{-1} K^{-1}) is the heat capacitance of skin; T_{pn} (in K) is the temperature of the treated section of skin immediately after the treatment; T_{pi} (in K) is the temperature of the treated section of skin immediately after pulse delivery. To calculate the temperature of the skin during cooling between pulses, we used the Lumped Capacitance Heat Conduction approximation as follows:

$$T_{cn} = T_{env} + (T_{pn} - T_{env})e^{-BiFo} \tag{3}$$

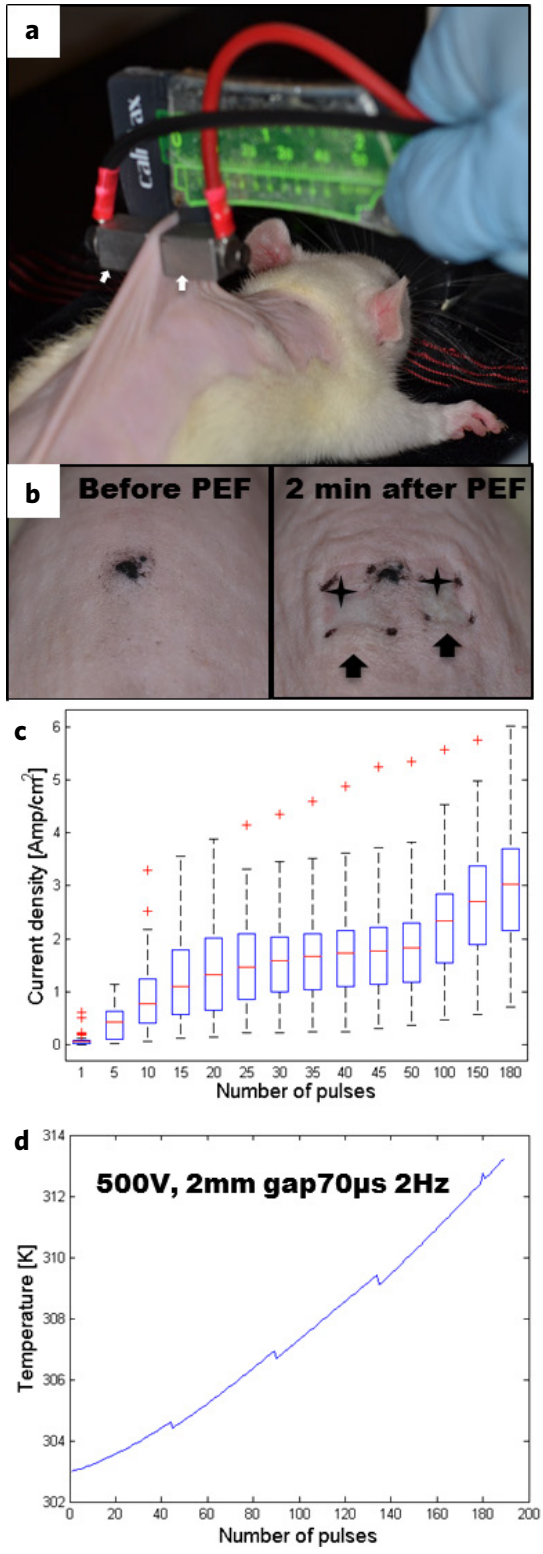

Figure 1 Pulsed electric field ablation of rat skin. (**a**) Experimental setup for PEF procedure. Contact electrodes (arrows) are applied on the dorsal skin. (**b**) Morphological appearance of rat skin before the treatment (left panel) and 2 min after PEF treatment (right panel). Skin edema is marked with arrows. Ischemia at the electrodes points of contact is marked with stars. (**c**) Box plot of current densities (Amp cm^{-2}) for each pulse (41 independent measurements per pulse are summarized). (**d**) Calculated skin temperature increase in Kelvin (K).

where T_{cn} (in K) is the temperature of the treated skin after a cooling period that followed pulse number (n); T_{env} (in K) is the environmental temperature; Bi is the Biot number and Fo is the Fourier number. (The justification for using this approximation appears in the **Supplementary Information 1**).

Solving Equations (1)−(3) simultaneously, we calculated the temperature increase of the treated rat skin during the PEF procedure (**Fig. 1d**). The modeling results (**Fig. 1d**) show that skin temperature did not increase more than 10 K (to ~40°C for a few minutes) during the entire treatment. Although, this temperature increase will not lead to cell death, it could possibly induce a weak heat shock response[15], which in turn might help preserve tissue structures and promote regeneration. In regards to future studies of PEF in tumor ablation, some effort should be placed on elucidating the effects of mild temperature increases on the tissue response to PEF, as they may impact the therapeutic outcome.

Gross examination of the PEF treated areas, 2 min after ablation, showed edema (**Fig. 1b, left panel arrows**) and localized ischemia (**Fig. 1b, left panel stars**), both of which subsided after 8 hours. Histopathological analysis of skin samples, harvested 24 hours after PEF, showed increased granulocytic infiltration (**Fig. 2a,d,e, arrows**). These infiltrates were temporary and resolved by 3 weeks (**Fig. 2a**). Further microscopic examination demonstrated rupture and scab formation in the epidermal layer (**Fig. 2d,e**), as well as sebaceous gland cell fusion and death (**Fig. 3d**) and death of hair follicles (**Fig. 3d,e**). At this time, the panniculus carnosus showed disintegration and death of skeletal muscle fibers as well as a massive infiltration of granulocytes (**Fig. 3d**). In spite of the massive damage to the PEF ablated areas, the ECM appeared intact (**Fig. 3e**).

To evaluate the effects of PEF on skin perfusion, we measured the local blood flow using laser Doppler imaging (LDI). LDI measures the perfusion rate in arbitrary units [Flux]. For analysis, we compared the ratio of Flux at the treated area to the Flux of untreated skin. A third-degree burn injury of similar area was generated as a positive control, normal skin at the same area before the treatment was used as a negative control. In this case, there was a marked difference in the perfusion pattern after PEF compared to the normal skin. Twenty four hours after injury, the Flux ratio in the third-degree burn area decreased to 0.3. In contrast, the PEF ablated area showed a 1.6 increase in the Flux ratio, indicating a preservation of blood supply and a hyperemic response (**Fig. 2b,c**). The preservation of blood supply to the PEF treated areas is consistent with previous reports, showing that PEF spares large blood vessels and major tissue structures[10−13]. These results differentiate PEF from radiofrequency and cryoablation, which do not preserve the blood supply to the ablated areas.

Unlike a third-degree burn which forms an eschar after a few days, PEF ablated tissue did not. In addition, the burn wounds after 2 months showed obvious signs of wound contracture while the PEF-treated areas did not. One week after PEF injury, we observed a thickened spinous layer with multiple cell layers, re-growth of sebaceous glands and hair follicles (**Supplementary Information 2**), multiple regenerating skeletal muscle fibers with centrally located nuclei (**Fig. 4b**), as well as a diminished granulocytic infiltrate to the panniculus carnosus (**Fig. 2a,4b**).

Two months post-injury with PEF, the epidermal spinous layer showed 1-2 layers of cells, which is equivalent to the thickness of normal skin (**Fig. 3a,b,e,f**). In addition, sebaceous glands and hair follicles were fully regenerated (**Fig. 3a,b,e,f**). The ECM appeared similar in both PEF-treated skin and untreated skin (**Fig. 3b,f**). In addition, we observed fusion of muscle fibers as well as migration of the nucleui to the periphery of these fused fibers in the panniculus

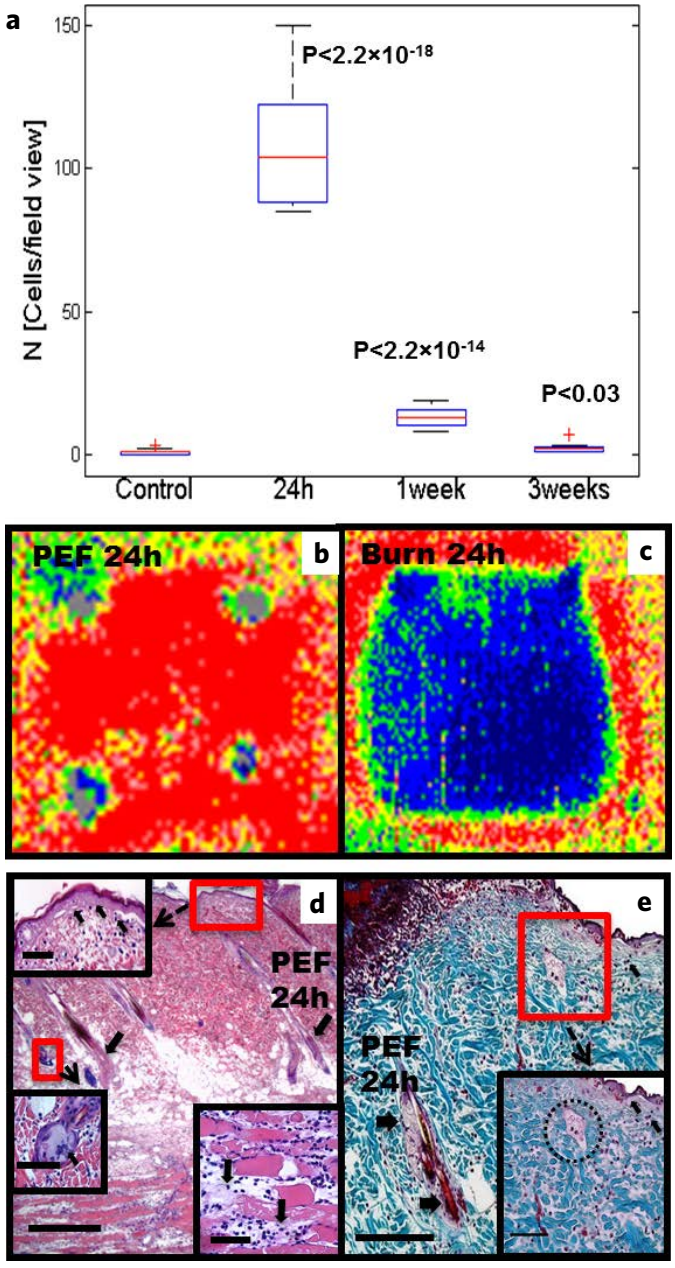

Figure 2 PEF induced damage to rat skin. (**a**) Dynamics of granulocytic infiltrate into PEF-treated areas at various time-points (number of cells/field of view). Boxplot analysis: 5 animals were used per time point, 3 sections per animal were counted. P-value was calculated using Student's t-test, comparing treated versus untreated samples. (**b,c**) Representative laser Doppler images of the dorsum of one Sprague-Dawley rat 24 hours post-injury. The small gray foci in each picture represent ink skin markings used to demarcate the treated areas. Low or no perfusion is displayed as dark blue, whereas the highest perfusion interval is displayed as red. (**b**) PEF, (**c**) third-degree burn. (**d,e**) Histological analysis of skin damage 24 hours after PEF ablation. (**d**) Shown is massive damage to the epidermis (decellularization is seen on the insert, emphasized by an arrow), hair follicles (arrows in the main image), panniculus carnosus (fiber-degradation is emphasized on the insert), and sebaceous gland fusion (insert, arrows shows multiple fused nuclei). (**e**) Masson's trichrome demonstrating that PEF preserves the collagen structure. Epidermis, hair follicles (arrows) and sebaceous glands (demarcation) are damaged. Scale bars: (**d**) = 500 μm, (**e**) = 250 μm, inserts = 200 μm.

carnosus two months post-injury with PEF (**Fig. 4c**). Most importantly, no signs of scar tissue formation were evident as collagen maintained its normal architecture. In contrast, third-degree burns did not show regeneration of sebaceous glands and hair follicles; moreover, collagen architecture was completely lost with fibers of similar diameter oriented parallel to the skin surface (**Fig. 3b–d,f**), and the epidermis was composed of multiple cell layers (**Fig. 3**).

Although the exact mechanisms of scarless tissue regeneration following PEF remain unclear and both necrosis and delayed apoptosis at the treated sites have been reported[8], we hypothesize that this regeneration is primarily due to the fact that PEF preserves the blood supply (**Fig. 2b**) and spares the ECM (**Fig. 2e**). Presumably, the preservation of the blood supply facilitates the supply of oxygen, nutrients, signaling molecules and cells to the PEF-damaged areas. This phenomenon is radically different from that seen in thermal burns or hypothermia induced tissue damage where the ECM structure is damaged, blood vessels thrombose and collapse, thus, preventing the transport of nutrients and regenerative components to the injured site.

In summary, we have shown that PEF-treatment results in acute cellular death and transiently altered skin perfusion, followed by a self-limited local inflammatory response. Despite early signs of

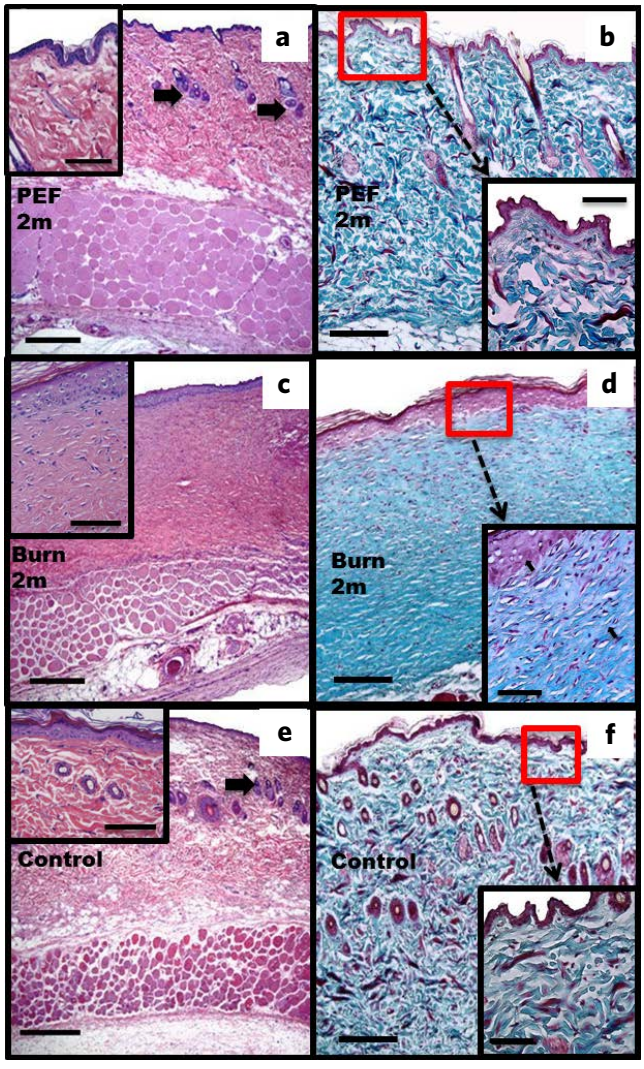

Figure 3 Histological analysis of rat skin after two months. (**a,b**) PEF injury. Shown is complete regeneration of structural and cellular skin components (**a**), Masson's trichrome (**b**), complete restoration of epidermal spinous layer with 1–2 cell layers ((**a**), insert), hair follicles and sebaceous glands ((**a**) arrows). Collagen fiber structure is similar to the untreated skin ((**b**) vs (**f**) inserts). (**c,d**) Third-degree burn. Absence of skin structures such as hair follicles and sebaceous glands (**c**), Masson's trichrome (**d**). Multicellular epidermis ((**c**), insert). The collagen fibers are parallel (arrows) and have a different structure compared to regular skin ((**b**) vs (**f**) inserts). (**e,f**) Untreated skin (**e**), Masson's trichrome (**f**). Skin structures are shown with arrows (**e**). Normal-layered epidermis ((**e**), insert). Normal structure of collagen is shown in (**f**). Scale bars: (**a,c,e**) = 500 μm; (**b,d,f**) = 250 μm; inserts = 200 μm.

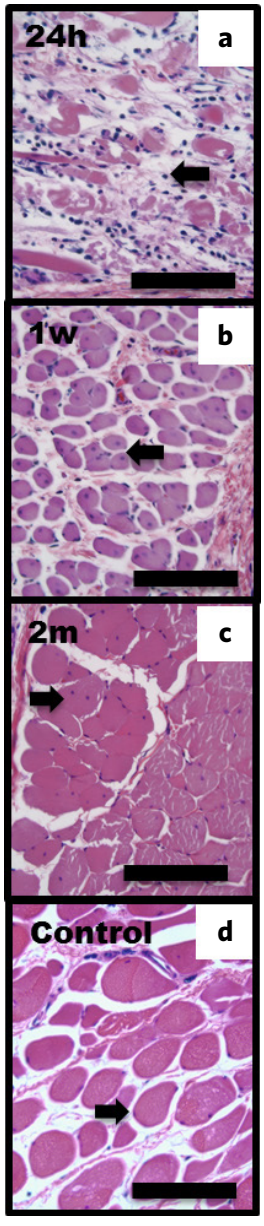

Figure 4 PEF induced damage and regeneration to the panniculus carnosus (H&E). (**a**) 24 h post-treatment. Infiltrating cell is shown by arrow. (**b**) Muscle fiber regeneration after one week. Single-nucleus cell of a regenerating fiber is shown by arrow. (**c**) Muscle regeneration two months after treatment. Regenerated fused fibers with a single nucleus in the center are shown by arrow. (**d**) Untreated muscle fibers. Scale bar = 100 μm.

significant tissue damage, complete skin and panniculus carnosus tissue regeneration without any signs of fibrosis is observed. These findings are strikingly different compared to thermal injuries, which typically lead to scar formation. Thus, PEF offers a highly promising strategy for scarless tissue regeneration.

ACKNOWLEDGEMENTS

We acknowledge MGH Fund for Medical Discovery for an ECOR postdoctoral fellowship award and Shriners Grant #85120-BOS for the support of this study. We also thank The Rodent Histopathology Core at Harvard Medical School and Dr. Roderick Terry Bronson for the support of this study.

COMPETING INTERESTS STATEMENT

The authors declare that they have no competing interests.

METHODS

Animals

Six-week-old female Sprague-Dawley rats (~200 g, N = 23) were obtained from Charles River Laboratories (Wilmington, MA). The animals were housed in individual cages with access to food and water ad libitum, and were maintained on a 12-hour light/dark cycle in a temperature controlled room. All animal procedures were approved by the Subcommittee on Research Animal Care (IACUC) of the Massachusetts General Hospital and were in accordance with the guidelines of the National Institutes of Health (NIH).

Pulsed electric fields

Prior to PEF treatment, animals were anesthesized with isoflurane. Their fur was clipped along the dorsal surfaces and treated with depilatory cream (Sally Hansen® Div. Del Laboratories, Inc., Farmingdale. NY). Subsequently, a designated area was subjected to electroporation using contact electrodes with a surface area of 1 cm^2. PEF specifications are as follows: 4 series × 45 pulses, pause of 30 s between treatment series, 500 V, 2mm gap between the electrodes, 70 µs duration, 2 Hz. Square pulses were delivered using BTX 830 pulse generator (Harvard Apparatus Inc, Holliston MA, USA). Currents were measured *in vivo* using PicoScope 4224 Oscilloscope with Pico Current Clamp (60A AC/DC) and analyzed with Pico Scope 6 software (Pico technologies Inc., UK). To evaluate temperature effects of PEF, heat transfer analysis was performed with MATLAB, R2009b (MathWorks, Natick, MA, USA). To construct a function that describes current density as a function of pulse numbers, a symbolic regression analysis was performed with Eureqa II (Cornell Creative Machines Lab). Pain was accessed twice daily, and buprenorphine (0.05 mg/kg) SQ/IM was given as needed for the first 72-h postprocedure period.

Burn injury

Before the creation of third-degree burns, the animals were anesthetized with isoflurane and their fur was clipped along the dorsal surfaces. Burns were incurred by pressing the ends of two pre-heated (≥ 95°C) brass blocks against opposite sides of a raised skin-fold from the rats dorsum for 10 seconds, resulting in a non-lethal, full-thickness, third-degree burn measuring approximately 1 cm^2. Burn injury and PEF were performed on the same animals on sites 2 cm apart from each other.

Laser Doppler scanning

A laser Doppler imager (Moor Instruments, Wilmington, DE) was used to assess blood flow. The laser Doppler source was mounted on a movable rack exactly 20 cm above the dorsum of the rat after the animal was anesthetized and restrained on the underlying table. The laser beam (780 nm) reflected from circulating red blood cells in capillaries, arterioles, and venules was detected and processed to provide a computerized, color-coded image. By using image analysis software (Laser Doppler Perfusion Measure, Version 3.08; Moor Instruments), mean flux values representing blood flow were calculated from the relative flux units for the areas corresponding to the dorsum of the rats. Baseline images were obtained from each rat before treatment was administered. Then, the rats were treated with either by PEF or a third-degree burn, and serial laser Doppler images were obtained subsequently. The entire procedure was done under warm conditions.

Histology

Specimens were harvested after 24 hours, 1 week, 3 weeks, and 2 months following the initial treatment. Five animals were euthanized for each time point. Three animals were used as controls. Skin samples were fixed in 10% formalin, embedded in paraffin, and cut into 5-um sections. Sections were stained with hematoxylin and eosin (H&E) and Masson's trichrome. Tissues were processed and stained by the Rodent Histopathology Core at Harvard Medical School. Slides were evaluated by three separate investigators, including an experienced dermatopathologist. Samples were imaged using Nikon Eclipse 800 and SPOT (version 4.0.9) camera (Diagnostic Instruments Inc, MI, USA).

Quantification of inflammatory response

To quantify the inflammatory reaction incurred by the panniculus carnosus of the PEF ablated areas, granulocytes were counted manually by two independent investigators. Three fields of view were imaged from slides for each animal (5 animals per time point). Cell counts were conducted using ImageJ (NIH, MD, USA).

Statistical analysis

Statistical analysis was performed with toolbox in MATLAB, R2009b (MathWorks, Natick, MA, USA). In order to fit the function for the current density changes over the number of pulses non-parametric regression analysis with Eureqa II (Cornell Creative Machines Lab, USA) was used. Five searches were performed for 4.5 h and ~1.2 M generations of functions. The chosen function showed the best error to complexity ratio. The confidence for the chosen function was: stability 8.64%, maturity 90.2%.

REFERENCES

1. Zhu, Z., Ding, J., Shankowsky, H.A. & Tredget, E.E. The molecular mechanism of hypertrophic scar. *J. Cell Commun. Signal.* **[Epub ahead of print]** (2013).
2. Koh, T.J. & DiPietro, L.A. Inflammation and wound healing: The role of the macrophage. *Expert Rev. Mol. Med.* **13**, e23 (2011).
3. Widgerow, A.D. Cellular/extracellular matrix cross-talk in scar evolution and control. *Wound Repair Regen.* **19**, 117–133 (2011).
4. Wong, V.W. *et al.* Focal adhesion kinase links mechanical force to skin fibrosis via inflammatory signaling. *Nat. Med.* **18**, 148–152 (2012).
5. Rowlatt, U. Intrauterine wound healing in a 20 week human fetus. *Virch. Arch.* **381**, 353–361 (1979).

6. Song, F., Li, B. & Stocum, D.L. Amphibians as research models for regenerative medicine. *Organogenesis* **6**, 141–150 (2010).
7. Ramos, M.L., Gragnani, A. & Ferreira, L.M. Is there an ideal animal model to study hypertrophic scarring? *J. Burn Care Res.* **29**, 363–368 (2008).
8. Golberg, A.Y. & Yarmush, M.L. Nonthermal irreversible electroporation: Fundamentals, applications, and challenges. *IEEE Trans. Biomed. Eng.* **60**, 707–714 (2013).
9. Narayanan, G. Irreversible electroporation for treatment of liver cancer. *Gastroenterol. Hepatol.* **7**, 313–316 (2011).
10. Maor, E., Ivorra, A., Leor, J. & Rubinsky, B. The effect of irreversible electroporation on blood vessels. *Technol. Cancer Research & Treatment* **6**, 307–312 (2007).
11. Phillips, M.A., Narayan, R., Padath, T. & Rubinsky, B. Irreversible electroporation on the small intestine. *Br. J. Cancer* **106**, 490–495 (2012).
12. Charpentier, K.P. *et al.* Irreversible electroporation of the pancreas in swine: A pilot study. *HPB (Oxford)* **12**, 348–351 (2010).
13. Rubinsky, B., Onik, G. & Mikus, P. Irreversible electroporation: A new ablation modality — clinical implications. *Technol. Cancer Res. Treat.* **6**, 37–48 (2007).
14. Golberg, A., Bei, M., Sheridan, R.L. & Yarmush, M.L. Regeneration and control of human fibroblast cell density by intermittently delivered pulsed electric fields. *Biotechnol. Bioeng.* **110**, 1759–1768 (2013).
15. Moloney, T.C., Hoban, D.B., Barry, F.P., Howard, L. & Dowd, E. Kinetics of thermally induced heat shock protein 27 and 70 expression by bone marrow-derived mesenchymal stem cells. *Protein Sci.* **21**, 904–909 (2012).

SUPPLEMENTARY INFORMATION 1: TEMPERATURE EFFECTS OF PULSED ELECTRIC FIELDS

To evaluate the temperature effects of pulsed electric fields (PEF) we developed a following electo-thermal model.

Geometry

PEF was delivered using contact electrodes we ablated a surface area (A) of 0.0001 m^2 of a dorsal skin of Sprague Dawley female rats. During the treatment, the skin was clamped between the electrodes as appears on **Fig. 1a**. The distance between the electrodes (L) was 0.002 m. Skin density was approximately 1100 (kg m^{-3}); therefore, the mass of a treated skin section was calculated as follows in Equation (S1):

$$m = A\rho L. \tag{S1}$$

Electro-thermal model of skin heating by pulsed electric fields

The heat supplied to the skin by each electric pulse is calculated as appears in Equation (S2):

$$Q = I(n)Vt_p \tag{S2}$$

where Q (Joule) is the heat supplied to the skin by each pulse (n); I(Amp) is the current during the pulse, V (Volt) is the applied voltage. Currents during each pulse were measured for the 40 animals (**Fig. 1c**). To model the effects of electric fields, we used non-parametric regression (described in the Methods section) to construct the equation that described current (I) as a function of pulse number (n). The derived expression appears in Equation (S3):

$$I(n) = 0.482n^{0,352}. \tag{S3}$$

The temperature increase of a treated skin section, immediately after the application of electric field is calculated using Equation (S4):

$$T_{pn} = \frac{Q}{mc_p} + T_{in} \tag{S4}$$

where m (gr) is the mass of a skin section on which electric fields are applied; c_p is the heat capacitance of skin; T_{pn} (K) is the temperature of the treated section of skin immediately after the treatment; T_{pi} (K) is the temperature of the treated section of skin immediately after pulse delivery.

The thermal properties of skin used in this model, and the initial conditions appear in Table 1S.

Next, to decide on the heat conduction model, we calculated the Biot number as appears in Equation (S5):

$$Bi = \frac{hL}{2k}. \tag{S5}$$

The calculated Biot number in this problem is 0.01; therefore, we used Lumpted Capacitance Heat Conduction approximation as follows:

$$T_{cn} = T_{env} + (T_{pn} - T_{env})e^{-BiFo} \tag{S6}$$

where T_{cn} (K) is the temperature of the treated skin (with N pulses) section after a cooling period; T_{env} (K) is the environmental temperature; Bi is Biot number and Fo is Fourier number, calculated as appears in Equation (S7):

$$Fo = \frac{kt}{\rho c_p (L/2)^2}. \tag{S7}$$

To obtain the temperature of skin during PEF treatment we solved Equations (S2)–(S4) and (S6) simultaneously for 180 pulses, delivered in groups of 45 at 2 Hz with a pause of 30 s between the groups.

FURTHER READING

1. Holmes, K.R. in *Heat and Mass Transfer in Living Systems*. (ed. K.R. Diller) 18–20 (N.Y. Acad. Sci., 1998).
2. Holmes, K. Thermal properties. http://users.ece.utexas.edu/~valvano/research/Thermal.pdf. (1998).
3. Kurazumi, Y. *et al.* Radiative and convective heat transfer coefficients of the human body in natural convection. *Build. Environ.* **43**, 2142–2153 (2008).
4. Shuangxi, H., Chunli, F., Li, Y., Sun, F. & Wei, K. in *Advanced Computational Intelligence (IWACI)*, 2011 Fourth International Workshop on 447–451 (2011).
5. Stewart, D.A., Gowrishankar, T.R. & Weaver, J.C. Skin heating and injury by prolonged millimeter-wave exposure: Theory based on a skin model coupled to a whole body model and local biochemical release from cells at supraphysiologic temperatures. *IEEE Trans. Plasma Sci.* **34**, 1480–1493 (2006).

Table 1S Skin thermal properties and environmental conditions during the experiment.

Model parameter	Sign	Value	Ref.
Rat skin heat capacitance (J kg^{-1} K^{-1})	c_p	3000	based on[1,2]
Convection heat transfer coefficient (W m^{-2} K^{-1})	h	4	based on[3]
Skin thermal conductivity (W m^{-1} K^{-1})	k	0.4	based on[2,4,5]
Environmental temperature (K)	T_{env}	298	measured
Initial temperature of the skin before treatment (K)	T_{in}	303	measured

SUPPLEMENTARY INFORMATION 2: SKIN REGENERATION 1 WEEK AFTER NON-THERMAL PEF ABLATION

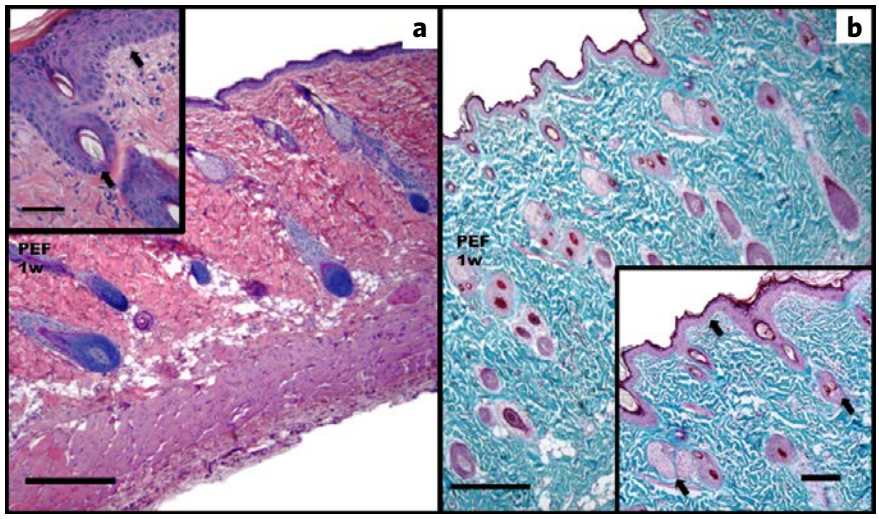

Figure S2 Histological analysis of rat skin 1 week after PEF. (**a**) H&E staining. Shown is regeneration of epidermis (insert arrows), hair follicles (insert arrows) and sebaceous glands (arrows). Epidermis is multilayer (insert arrows). No significant inflammatory infiltration is observed. Scale bars: 500 μm, insert 200 μm. (**b**) Masson's trichrome stain. The collagen network structure is similar to normal skin (**Fig. 3f**). Regenerating sebaceous glands and hair follicles are shown by arrows in the insert. Scale bars: 250 μm, insert 200 μm.